

HUMAN-LLM COLLABORATIVE FEATURE ENGINEERING FOR TABULAR LEARNING

Zhuoyan Li¹, Aditya Bansal², Jinzhao Li¹, Shishuang He³, Zhuoran Lu¹,
Mutian Zhang¹, Yiwei Yang⁴, Qin Liu⁵, Swati Jain², Ming Yin¹, Yunyao Li²

¹Purdue University ²Adobe ³UIUC ⁵University of Washington ⁴UC Davis

ABSTRACT

Large language models (LLMs) are increasingly used to automate feature engineering in tabular learning. Given task-specific information, LLMs can propose diverse feature transformation operations to enhance downstream model performance. However, current approaches typically assign the LLM as a black-box optimizer, responsible for both proposing and selecting operations based solely on its internal heuristics, which often lack calibrated estimations of operation utility and consequently lead to repeated exploration of low-yield operations without a principled strategy for prioritizing promising directions. In this paper, we propose a human-LLM collaborative feature engineering framework for tabular learning. We begin by decoupling the transformation operation proposal and selection processes, where LLMs are used solely to generate operation candidates, while the selection is guided by explicitly modeling the utility and uncertainty of each proposed operation. Since accurate utility estimation can be difficult especially in the early rounds of feature engineering, we design a mechanism within the framework that selectively elicits and incorporates human expert preference feedback—comparing which operations are more promising—into the selection process to help identify more effective operations. Our evaluations on both the synthetic study and the real user study demonstrate that the proposed framework improves feature engineering performance across a variety of tabular datasets and reduces users’ cognitive load during the feature engineering process.

1 INTRODUCTION

Today, AI-powered models are increasingly integrated into diverse applications, such as fraud detection (Yang et al., 2025) and online platform recommendation (Alfaifi, 2024; Resnick & Varian, 1997), where tabular data remains one of the most popular data modalities to represent structured information like financial transaction logs or user profiles Nam et al. (2023). The quality of the feature engineering, which transforms raw feature columns into meaningful representations, often plays a critical role in determining the performance of AI models. To reduce manual effort in the feature engineering, traditional AutoML-based methods (Zhang et al., 2023; Erickson et al., 2020) have been developed to automate feature construction by applying predefined transformation operators over feature columns, which often lack the task-specific understanding and tend to generate redundant features that lead to suboptimal model performance.

Recent advances in large language models (LLMs) (Achiam et al., 2023), with their strong language understanding and reasoning abilities, have motivated numerous studies to directly apply LLMs in feature engineering for tabular prediction tasks, aiming to leverage their semantic understanding to create informative features to improve the downstream model performance (Bordt et al., 2024; Han et al., 2025). For example, CAAFE (Hollmann et al., 2023) uses the task description together with the semantic description of each feature to prompt an LLM to iteratively synthesize semantically meaningful features. Nam et al. treats the LLM as a black-box optimizer that proposes and refines feature generation rules using feedback from the validation score of the downstream AI model and the verbalized reasoning distilled from a fitted decision tree. Although these approaches can improve performance, the current approaches typically assign the LLM both the role of proposing feature transformation operations and the role of selecting among them, so that the entire process is driven purely by the model’s internal heuristics, which often lacks calibrated estimates of the utility and the

uncertainty of each operation and in turn can lead to repeated exploration of low-yield operations without a principled strategy for prioritizing more promising directions. As a result, it tends to waste evaluation budget on low-yield transformations and performs poorly when the number of feature engineering iterations is limited.

In this paper, we propose a human–LLM collaborative feature engineering framework for tabular learning. We begin by decoupling the transformation operation proposal and selection processes, where LLMs are used solely to propose diverse transformation operation candidates based on their internal heuristics and understanding of the current task, while the selection is guided by explicit modeling of the utility and uncertainty of each proposed operation. However, the estimated utility of feature operations can often be poorly calibrated against their actual utility, particularly in the early rounds of feature engineering when only limited observational data is available to fit the estimation model. In such cases, human expert collaborators (e.g., machine learning practitioners), who have accumulated domain knowledge about which types of feature transformations are likely to be beneficial, can provide qualitative insights to support more informed selection among the LLM-proposed feature operations. To incorporate such qualitative knowledge into the selection process in a tractable manner, following prior work (AV et al., 2022; Xu et al., 2024a), we consider the form of *preference feedback*¹ from the human, where they compare pairs of feature operations to indicate which is better. To effectively leverage this form of human preference feedback without incurring excessive human cognitive cost, we design a mechanism within the framework that selectively elicits preference feedback from the human collaborator only when the potential gain from the human feedback can justify this additional human effort. To evaluate the effectiveness of the proposed framework, we first conducted a synthetic study across a variety of tabular datasets. Compared to different baselines including both AutoML methods and LLM-powered feature engineering methods, our method exhibits consistent improvement when evaluated with different downstream models. We then conducted a user study to further understand how actual users collaborate with the LLM in our framework. We observed that our algorithm can also improve the actual feature engineering performance and reduce the cognitive load experienced by human experts during the process.

2 RELATED WORK

Large Language Models (LLMs) for Tabular Learning. Recent advances in large language models (LLMs) (Achiam et al., 2023), with their strong language understanding and reasoning abilities, have motivated numerous studies to apply LLMs to tabular prediction tasks (Wang et al., 2023; Ko et al., 2025; Bouadi et al., 2025; Zhang et al., 2024; Han et al., 2024; Nam et al., 2024b). One line of work adapts LLMs by converting structured and tabular data into natural language and then leveraging zero- or few-shot inference or fine-tuning of LLMs (Dinh et al., 2022; Hegselmann et al., 2023; Yan et al., 2024). More recently, researchers have explored using LLMs to directly propose and select new features from the original feature columns and task descriptions to augment predictive performance (Hollmann et al., 2023; Bordt et al., 2024; Han et al., 2025; Abhyankar et al., 2025). For example, Nam et al. treats the LLM as a black-box optimizer which proposes and refines feature generation rules using feedback from the validation score of the downstream machine learning model and the verbalized reasoning distilled from a fitted decision tree. In this paper, we ask whether it is possible to decouple the generation and the selection process by explicitly modeling both the utility and the uncertainty of LLM-generated feature operations with Bayesian optimization, so as to guide the selection and composition of features in a more efficient and principled manner.

Human-AI Collaboration for Interactive Machine Learning. There has been a growing interest among researchers in leveraging human knowledge to enhance standard machine learning pipelines. Many studies investigate the factors that influence effective human–AI collaboration (Lai et al., 2021; Buçinca et al., 2021; Chiang et al., 2023; 2024). For example, Wang et al. conducted interviews with industry practitioners to understand their experiences with AutoML systems. Some recent work has focused on redesigning the interaction between humans and models during the learning process (Mozannar et al., 2023; Wei et al., 2024; De Toni et al., 2024; Alur et al., 2024). In this line of research, collaboration is operationalized through mechanisms such as modifying the objective functions to promote human-AI complementarity (Bansal et al., 2019a;b; Mahmood et al.,

¹As shown in prior research (Kahneman & Tversky, 2013), this pairwise preference format enables humans to more effectively express their internal judgments compared to directly evaluating individual instances.

2024), adjusting how to present information like AI confidence or explanation based on the human behavior modeling (Vodrahalli et al., 2022; Li & Yin, 2024; Li et al., 2024; Lu et al., 2023; Li et al., 2023b; 2025), and reducing human workload by shifting their role from primary decision maker to on-demand advisor, typically through selective querying paradigms that solicit human input only when it is expected to be most valuable (AV et al., 2022; Xu et al., 2024a;b; Souza et al., 2021; Hvarfner et al., 2022). In this paper, we ask how human expertise should inform and shape the LLM-powered feature engineering process in order to achieve more complementary outcomes.

3 METHODOLOGY

3.1 MOTIVATION AND PROBLEM FORMULATION

In this study, we explore the scenario of human–LLM collaborative feature engineering in supervised tabular prediction tasks, and we now formally describe it. Let $\mathcal{D} = \{(\mathbf{x}_i, y_i)\}_{i=1}^n$ denote the tabular dataset, where each $\mathbf{x}_i \in \mathbb{R}^d$ is a d -dimensional feature vector for the task instance, and the j -th dimension corresponds to a feature column with name $c_j \in C = \{c_1, \dots, c_d\}$. The label y_i is the target output, with $y_i \in \{0, 1, \dots, K\}$ for a K -class classification task and $y_i \in \mathbb{R}$ for a regression task. By splitting the dataset \mathcal{D} into the training set $\mathcal{D}_{\text{train}}$ and the validation set \mathcal{D}_{val} , a tabular learner f_{tabular} is trained on $\mathcal{D}_{\text{train}}$ and evaluated on \mathcal{D}_{val} by a task-appropriate score function $J(f_{\text{tabular}}; \mathcal{D}_{\text{val}})$ (e.g., AUCROC for classification task, and negative MSE for regression task). Let Φ denote the space of candidate feature transformation operations. Each operation $e \in \mathcal{E}$ maps the original data matrix $\mathcal{X} \in \mathbb{R}^{n \times d}$ into a new feature column $z_e \in \mathbb{R}^n$. The updated training and validation datasets are represented as $\mathcal{D}_{\text{train}} \oplus e$ and $\mathcal{D}_{\text{val}} \oplus e$, respectively, where \oplus represents the addition of the new feature column z_e to the existing dataset. To evaluate the utility of a feature operation e , we first define the black-box utility function $g(\cdot)$:

$$g(e) = J(f_{\text{tabular}}; \mathcal{D}_{\text{val}} \oplus e), \quad \text{where} \quad f_{\text{tabular}} = \arg \min_f \mathcal{L}(f; \mathcal{D}_{\text{train}} \oplus e) \quad (1)$$

Here, \mathcal{L} is the loss function used to train the tabular learner (e.g., cross-entropy for classification or MSE for regression). Since feature engineering proceeds in multiple rounds, where at each round t , we evaluate the utility of a selected transformation e_t , and update $\mathcal{D}_{\text{train}}$ and \mathcal{D}_{val} only if $g(e_t) > 0$. The goal of feature engineering in each round is to identify the operation that maximizes predictive performance on the current validation set :

$$e_t^* = \arg \max_{e \in \mathcal{E}} g(e) \quad (2)$$

However, the utility function $g(\cdot)$ is observable only after an expensive refit and re-evaluate cycle on the updated model. Prior work on LLM-powered feature engineering (Hollmann et al., 2023; Nam et al., 2024a) addresses this black-box optimization by treating the LLM as an implicit surrogate for $g(\cdot)$, with the LLM M handling both proposal and selection of the optimal transformation e^* . In round t of feature engineering process, given the observed performance history $H_t = \{(e_i, g(e_i))\}_{i=1}^{t-1}$, column descriptions C , and dataset-level metadata including the prediction objective Meta, the LLM samples a set of N candidates $\mathcal{S}_t = \{e_t^1, \dots, e_t^N\}$ from its internal proposal distribution:

$$\mathcal{S}_t \sim \mathcal{P}_M(\cdot \mid H_t, C, \text{Meta}) \quad (3)$$

The LLM M would then select a candidate $e_t \in \mathcal{S}_t$ based on internal heuristics about which transformation might be most useful in the current round. In this paper, we ask whether it is possible to de-couple transformation operation proposal and selection processes, where the LLM M serves solely as a operation proposal generator, sampling candidates from the distribution $\mathcal{P}_M(\cdot \mid H_t, C, \text{Meta})$, and the selection is guided by explicitly modeling the utility of LLM-proposed feature operations. To address the black-box nature of the utility function $g(\cdot)$, we adopt a Bayesian optimization approach that first constructs an explicit surrogate model $\hat{g}(\cdot)$ based on the history H_t to estimate the utility and uncertainty of each operation. Based on this surrogate model, we next move to explore how to select among the LLM-proposed candidate operations in each round, and how to selectively elicit and incorporate human preference feedback into the model selection process.

3.2 SURROGATE MODEL FOR APPROXIMATION OF THE UTILITY FUNCTION $g(\cdot)$

In this part, we describe how to construct a surrogate model $\hat{g}(\cdot)$ to approximate $g(\cdot)$.

Encoding of LLM-Proposed Feature Operations. To allow the surrogate model to effectively approximate the utility function $g(\cdot)$, each LLM-proposed feature transformation e is first mapped into a vector representation. We first apply a pretrained embedding encoder $\phi_{\text{embedding}}(e)$ ² to obtain a dense semantic representation of the operation e , which captures compositional and linguistic relationships among candidate operations that are learnable by the surrogate model. However, the semantic embedding $\phi_{\text{embedding}}(e)$ alone may be insufficient when multiple feature columns have similar linguistic descriptions. To address this, we incorporate a column-usage encoder $\phi_{\text{column}}(e)$ to provide explicit structural information about which feature columns are used in the feature operation. Specifically, $\phi_{\text{column}}(\cdot)$ maps an operation e into a binary vector $\mathbf{m} \in \{0, 1\}^d$, where $\mathbf{m} = [\mathbb{I}[c_i \text{ is used in } e]]_{i=1}^d$ and each $c_i \in C$ denotes a column from the input data matrix. Finally, the overall embedding representation for the surrogate model \hat{g} is obtained by concatenating the two components:

$$\phi(e) = [\phi_{\text{embedding}}(e), \phi_{\text{column}}(e)] \quad (4)$$

Bayesian Neural Network as Surrogate Model. In Bayesian optimization, Gaussian processes (GPs) are widely used as surrogate models in different tasks such as hyperparameter tuning (Snoek et al., 2012) and system design (Wang et al., 2024), which typically involve relatively simple, low-dimensional feature spaces that GPs can scale effectively (Xu et al., 2024c). In contrast, our setting requires modeling LLM-proposed feature operations that are expressed in natural-language format and mapped via an encoder $\phi(\cdot)$ into a high-dimensional representation, where GPs often struggle to scale and capture non-stationarity (Snoek et al., 2015). Therefore, in this paper, we opted for Bayesian neural network (BNN) as the surrogate \hat{g} , which can provide greater scalability and expressiveness for modeling high-dimensional, language-derived feature embeddings (Li et al., 2023a). Specifically, given the performance history at the current round $H_t = \{(e_i, g(e_i))\}_{i=1}^{t-1}$, the surrogate \hat{g} is constructed as a Bayesian neural network parameterized by θ , which defines a predictive model $\hat{g}(\phi(e); \theta)$ over candidate operations e to approximate their true utility $g(e)$. To capture uncertainty, instead of learning a single point estimate of θ , we adopt a Bayesian approach and set out to learn the posterior distribution of the model parameters conditioned on history H_t , i.e., $\mathcal{P}(\theta | H_t)$. As directly computing this posterior $\mathcal{P}(\theta | H_t)$ is intractable, we learn the variational distribution $q_t(\theta) = \mathcal{N}(\theta; \mathbf{M}_t, \Sigma_t)$ by minimizing the KL divergence between $q_t(\theta)$ and the true posterior:

$$\begin{aligned} \text{KL}(q_t(\theta) \| \mathcal{P}(\theta | H_t)) &= \int q_t(\theta) \log \frac{q_t(\theta)}{\mathcal{P}(\theta | H_t)} d\theta \\ &= \int q_t(\theta) \left(\log \frac{q_t(\theta)}{\mathcal{P}(\theta)} - \log \mathcal{P}(H_t | \theta) + \log \mathcal{P}(H_t) \right) d\theta \\ &= \text{KL}(q_t(\theta) \| \mathcal{P}(\theta)) - \mathbb{E}_{q_t(\theta)} [\log \mathcal{P}(H_t | \theta) - \log \mathcal{P}(H_t)] \end{aligned} \quad (5)$$

where $\mathcal{P}(\theta)$ is the prior distribution over model parameters and $\mathcal{P}(H_t)$ is a constant³. Given the learned variational posterior $q_t(\theta)$, the predicted *expected utility* $\mu_t(e)$ of a candidate operation e and its corresponding *uncertainty* $\sigma_t^2(e)$ are computed as:

$$\mu_t(e) = \mathbb{E}_{q_t(\theta)} [\hat{g}(\phi(e); \theta)], \quad \sigma_t^2(e) = \mathbb{E}_{q_t(\theta)} [\hat{g}(\phi(e); \theta)^2] - \mu_t(e)^2 \quad (6)$$

Lemma 3.1. *At round t , the LLM M proposes a set of candidate operations \mathcal{S}_t . For any $\delta \in (0, 1)$, with probability at least $1 - \delta$, the deviation between the actual utility $g(e)$ and the predicted expected utility $\mu_t(e)$ is uniformly bounded for all $e \in \mathcal{S}_t$.*

$$\mathbb{P}\left(\forall t \geq 1, \forall e \in \mathcal{S}_t : |g(e) - \mu_t(e)| \leq \sqrt{\beta_t} \sigma_t(e)\right) \geq 1 - \delta, \quad \beta_t = 2 \log\left(\frac{|\mathcal{S}_t| \pi^2 t^2}{3\delta}\right) \quad (7)$$

Proof sketch. Assuming the actual utility function $g(\cdot)$ can be linearly represented in the surrogate feature space $\phi(\cdot)$, the standardized error $(g(e) - \mu_t(e))/\sigma_t(e)$ is 1-sub-Gaussian, which gives the tail bound $\mathbb{P}(|g(e) - \mu_t(e)| > u \sigma_t(e)) \leq 2e^{-u^2/2}$. By applying a union bound over \mathcal{S}_t , we can then establish the confidence event in Equation. 7. The full proof is provided in Appendix A.1.

Given the predicted *expected utility* $\mu_t(e)$ and the *uncertainty* $\sigma_t^2(e)$ of each candidate operation e at round t of the feature engineering process, when human expertise is not available, the selection is solely based on the surrogate model's estimation. We adopt the Upper Confidence Bound (UCB) selection function (Auer et al., 2002; AV et al., 2022; Xu et al., 2024a) to balance exploitation of

²In this study, we instantiate $\phi_{\text{embedding}}$ with OpenAI's `text-embedding-3-small` model.

³In this study, we set $\mathcal{P}(\theta) = \mathcal{N}(\mathbf{0}, I)$ as the prior over network parameters.

high predicted utility and exploration of uncertain operations. Specifically, for each round $t \leq T$ and LLM-proposed candidate operation $e \in \mathcal{S}_t$, the UCB selection function is defined as:

$$\text{UCB}_t(e) = \mu_t(e) + \sqrt{\beta_t} \sigma_t(e) \quad (8)$$

where $\beta_t = 2 \log\left(\frac{|\mathcal{S}_t| \pi^2 t^2}{3\delta}\right)$ is set according to Lemma 3.1, which guarantees that, with probability at least $1 - \delta^4$, $g(e) \in [\text{LCB}_t(e), \text{UCB}_t(e)]$ for all $e \in \mathcal{S}_t$, where $\text{LCB}_t(e) = \mu_t(e) - \sqrt{\beta_t} \sigma_t(e)$.

3.3 SELECTION OF LLM-PROPOSED FEATURE OPERATIONS WHEN HUMAN EXPERTISE IS AVAILABLE

When the human collaborator is available, we next proceed to explore how to selectively elicit and incorporate their preference feedback into the selection process of LLM-proposed operations.

Selection of the Feature Operation Candidate Pair for Human Preference Feedback. Specifically, the human expertise in the feature engineering process is modeled as a stochastic oracle κ . At round t , given a pair of feature operations (e_t^a, e_t^b) , the oracle elicits a binary response $\kappa(e_t^a, e_t^b) = Z_t \in \{+1, -1\}$, where $Z_t = +1$ indicates $e_t^a \succ e_t^b$ and $Z_t = -1$ indicates $e_t^b \succ e_t^a$. We begin by describing how to select the pair (e_t^a, e_t^b) to obtain human feedback at each round t . If the human collaborator κ is not available at round t , we directly follow the UCB function (Equation 8) to select $e_t^a = \arg \max_{e \in \mathcal{S}_t} \text{UCB}_t(e)$ to evaluate in this round. When human expertise κ is available, an additional operation e_t^b can be selected from the remaining pool $\mathcal{S}_t \setminus \{e_t^a\}$ such that the preference feedback Z_t over the pair (e_t^a, e_t^b) yields the highest expected utility gain relative to the surrogate model’s current choice e_t^a . To define the expected information gain, let e_t^* denote the true optimal feature transformation at round t . The prior regret of the current selection is defined as $r_t = g(e_t^*) - g(e_t^a)$, which measures the utility gap between the surrogate’s choice e_t^a and the unknown optimum e_t^* . If we select another candidate e_t^b and query the human oracle κ to obtain preference feedback Z_t , we may revise the final decision to $e_t' \in \{e_t^a, e_t^b\}$ according to the feedback. The new regret becomes $r_t' = g(e_t^*) - g(e_t')$. Therefore, the expected utility gain is defined as the expected reduction in regret resulting from incorporating human preference into the selection process:

$$U(e_t^a, e_t^b; \kappa) = \mathbb{E}_{Z_t}[r_t - r_t'] = \mathbb{E}_{Z_t}[g(e_t') - g(e_t^a)] \quad (9)$$

Lemma 3.2. *By the Lemma 3.1, let $e_t^a \in \mathcal{S}_t$ be the UCB choice, the following holds for any operation $e_t^b \in \mathcal{S}_t \setminus \{e_t^a\}$ and $1 \leq t \leq T$:*

$$U(e_t^a, e_t^b; \kappa) = \mathbb{E}_{Z_t}[r_t - r_t'] \leq \max\{\text{UCB}_t(e_t^b) - \text{LCB}_t(e_t^a), 0\} \quad (10)$$

Proof sketch. Under the feature operation selection pair (e_t^a, e_t^b) , the human preference feedback can switch the round- t choice of feature operation between e_t^a and e_t^b , so $r_t - r_t' \leq \max\{g(e_t^b) - g(e_t^a), 0\}$. By Lemma 3.1, we have $g(e_t^b) \leq \text{UCB}_t(e_t^b)$ and $g(e_t^a) \geq \text{LCB}_t(e_t^a)$, which together gives the lemma. The full proof is provided in Appendix A.2.

Corollary 3.1. *By Lemma 3.2, we have:*

$$U(e_t^a, e_t^b; \kappa) \leq \max\{\text{UCB}_t(e_t^b) - \text{LCB}_t(e_t^a), 0\} \leq \sqrt{\beta_t}(\sigma_t(e_t^a) + \sigma_t(e_t^b)) \quad (11)$$

Based on Lemma 3.2, the candidate operation e_t^b is selected to be paired with e_t^a for human preference feedback:

$$e_t^b = \arg \max_{e \in \mathcal{S}_t \setminus \{e_t^a\}} \text{UCB}_t(e) \quad (12)$$

Selective Elicitation for Human Preference Feedback. However, since eliciting human feedback inevitably incurs cognitive costs and increases the expert’s workload, it is impractical to query the human collaborator in every round. Instead, feedback should be requested only when it is expected to yield gains that outweigh the associated costs, and incorporating human expertise can guide the selection algorithm toward more informed and effective decisions. Given the candidate pair $\{e_t^a, e_t^b\}$, we first consider whether human expert feedback has the potential to provide additional utility beyond the current selection. If $\text{UCB}_t(e_t^b) \leq \text{LCB}_t(e_t^a)$, then by Lemma 3.1, it indicates

⁴In this study, δ is set as 0.1 to control the confidence interval.

that $g(e_t^b) \leq g(e_t^a)$. In this case, the current feature operation e_t^a strictly outperforms the candidate e_t^b , leaving no possibility for human expertise to improve the utility further. To prevent this, our first condition requires that the two confidence intervals should overlap to ensure that there remains uncertainty about which operation is better, thereby leaving the “room” for human expertise to potentially improve the selection:

$$(C1) \text{ Overlap: } \text{UCB}_t(e_t^b) > \text{LCB}_t(e_t^a) \quad (13)$$

Even when overlap exists, however, not all human feedback are equally valuable. The second consideration is whether the underlying improvement of utility is sufficiently large to justify the cognitive cost of involving the expert. Let γ_κ denote the cost of eliciting human feedback in each round⁵. By Corollary 3.1, the maximum possible utility gain is upper-bounded by $\sqrt{\beta_t}(\sigma_t(e_t^a) + \sigma_t(e_t^b))$. To prevent unprofitable queries, we therefore impose the following requirement to guarantees the human feedback is only triggered when the potential utility improvement might outweigh the cost:

$$(C2) \text{ Uncertainty: } \sqrt{\beta_t}(\sigma_t(e_t^a) + \sigma_t(e_t^b)) \geq \gamma_\kappa \quad (14)$$

Taken together, the human feedback query is only elicited if and only if these two conditions hold:

$$(C1) \text{ Overlap: } \text{UCB}_t(e_t^b) > \text{LCB}_t(e_t^a) \quad \text{and} \quad (C2) \text{ Uncertainty: } \sqrt{\beta_t}(\sigma_t(e_t^a) + \sigma_t(e_t^b)) \geq \gamma_\kappa \quad (15)$$

Posterior Selection with Human Preference Feedback. Once the condition is satisfied and preference feedback $Z_t = \kappa(e_t^a, e_t^b)$ is elicited, the model distribution $q_t(\boldsymbol{\theta})$ for the surrogate model \hat{g} , which is constructed based on the past performance history H_t using Equation 5, serves as the model’s current belief about which feature operations may be useful. We then proceed to determine the final feature transformation for round t by integrating this model belief $q_t(\boldsymbol{\theta})$ with the elicited human preference Z_t . Instead of making a direct selection based on Z_t , we treat Z_t as a probabilistic observation that provides information about the relative utility between the two candidate operations. Specifically, the feedback likelihood is modeled using a probit function:

$$\mathcal{P}(Z_t | \boldsymbol{\theta}, e_t^a, e_t^b) = \Phi\left(\eta Z_t [\hat{g}(\phi(e_t^a); \boldsymbol{\theta}) - \hat{g}(\phi(e_t^b); \boldsymbol{\theta})]\right), \quad \text{where } \boldsymbol{\theta} \sim q_t(\boldsymbol{\theta}) \quad (16)$$

where $\Phi(\cdot)$ is the standard normal cumulative distribution function (CDF), and η is a hyperparameter that controls the confidence level of feedback⁶. Assuming that the elicited human feedback Z_t , derived from human expertise, is conditionally independent of the performance history H_t , the posterior distribution $q'_t(\boldsymbol{\theta})$ can be updated as:

$$\begin{aligned} \text{KL}(q'_t(\boldsymbol{\theta}) \| \mathcal{P}(\boldsymbol{\theta} | H_t, Z_t, e_t^a, e_t^b)) &= \int q'_t(\boldsymbol{\theta}) \log \frac{q'_t(\boldsymbol{\theta})}{\mathcal{P}(\boldsymbol{\theta} | H_t, Z_t, e_t^a, e_t^b)} d\boldsymbol{\theta} \\ &= \int q'_t(\boldsymbol{\theta}) \left(\log \frac{q'_t(\boldsymbol{\theta})}{\mathcal{P}(\boldsymbol{\theta} | H_t)} - \log \mathcal{P}(Z_t | \boldsymbol{\theta}, e_t^a, e_t^b) + \log \mathcal{P}(Z_t | H_t, e_t^a, e_t^b) \right) d\boldsymbol{\theta} \\ &\approx \text{KL}(q'_t(\boldsymbol{\theta}) \| q_t(\boldsymbol{\theta})) - \mathbb{E}_{q'_t(\boldsymbol{\theta})}[\log \mathcal{P}(Z_t | \boldsymbol{\theta}, e_t^a, e_t^b)] + \mathbb{E}_{q'_t(\boldsymbol{\theta})}[\log \mathcal{P}(Z_t | H_t, e_t^a, e_t^b)] \end{aligned} \quad (17)$$

With the updated posterior distribution $q'_t(\boldsymbol{\theta})$, we can then make the selection of the final feature operation to be evaluated for this round t :

$$e_t^{\text{selected}} = \text{argmax}_{e \in \{e_t^a, e_t^b\}} \text{UCB}_t(e) \quad (18)$$

Finally, Algorithm 1 summarizes how does the proposed framework perform the iterative selection of LLM-proposed feature transformation operations in the feature engineering process.

4 EVALUATIONS

4.1 EXPERIMENTAL SETUP

Dataset. Following previous work (Hollmann et al., 2023; Bordt et al., 2024), we select 18 datasets from Kaggle and UCI Irvine, which contain a mix of categorical and numerical features for classification or regression tasks. Since LLMs are trained on large-scale public data, which may include

⁵ γ_κ is empirically set to 4 in this study to balance the trade-off between final performance and efficiency for the elicitation of human feedback.

⁶ η is set as 1 in this study.

Table 1: Comparing the performance of the proposed method, LLM-based baselines, and non-LLM-based baselines on 13 classification datasets in terms of **AUROC (%)** with GPT-4o as the backbone model for all LLM-based methods, evaluated using MLP and XGBoost as the tabular learning models, respectively. The **best method** in each row is highlighted in **blue**, and the **best baseline method** is highlighted in **light blue**. The number in the brackets () indicate the error reduction rate compared to the **best baseline method**. All results are averaged over 5 runs.

Dataset	MLP					XGBoost						
	OpenFE	AutoGluon	CAAFE	OCTree	Ours (w/o human)	Ours (w/ human)	OpenFE	AutoGluon	CAAFE	OCTree	Ours (w/o human)	Ours (w/ human)
flight	93.3	92.6	92.9	94.8	96.9 (+0.4%)	97.3 (+48.1%)	95.7	95.4	95.2	96.4	97.6 (+33.3%)	98.0 (+44.4%)
wine	77.2	77.2	77.6	78.2	78.5 (+1.4%)	78.7 (+2.3%)	81.3	81.0	80.9	82.1	82.9 (+4.5%)	83.3 (+6.7%)
loan	95.3	95.4	95.7	95.9	96.0 (+2.4%)	96.1 (+4.9%)	96.2	96.0	96.1	96.5	96.9 (+11.4%)	97.1 (+17.1%)
diabetes	81.1	82.4	82.8	82.8	83.0 (+1.2%)	83.0 (+1.2%)	84.1	83.9	83.9	84.4	85.2 (+5.1%)	84.8 (+2.6%)
titanic	84.1	84.3	86.3	86.5	86.8 (+2.2%)	87.0 (+3.7%)	85.0	84.8	87.0	87.4	87.9 (+4.0%)	88.3 (+7.1%)
travel	80.4	80.3	81.1	81.7	82.0 (+1.6%)	82.3 (+3.3%)	83.6	83.2	83.6	84.6	85.3 (+4.5%)	85.7 (+7.1%)
ai-usage	67.8	67.5	68.2	68.0	68.5 (+0.9%)	68.3 (+0.3%)	71.8	71.5	71.3	72.4	73.3 (+3.3%)	73.8 (+5.1%)
water	53.7	53.2	56.7	57.9	58.7 (+1.9%)	59.3 (+3.3%)	56.7	56.1	59.8	61.7	63.2 (+3.9%)	64.1 (+6.3%)
heart	92.2	92.3	92.6	93.1	93.4 (+4.3%)	93.6 (+7.2%)	93.6	93.5	93.6	94.3	95.1 (+14.0%)	94.8 (+8.8%)
adult	90.5	90.4	90.8	90.9	91.3 (+4.4%)	91.4 (+5.5%)	91.6	91.3	91.5	92.0	92.4 (+5.0%)	92.8 (+10.0%)
customer	84.6	84.5	84.9	84.8	85.1 (+1.3%)	85.1 (+1.3%)	85.3	85.0	85.3	85.2	85.8 (+3.4%)	86.3 (+6.8%)
personality	94.4	94.1	95.0	95.4	96.1 (+15.2%)	96.1 (+15.2%)	96.4	96.2	96.6	97.1	97.4 (+10.3%)	97.6 (+17.2%)
conversion	90.7	90.6	90.9	91.1	92.6 (+16.9%)	92.9 (+20.2%)	91.2	91.9	92.1	92.4	93.5 (+5.7%)	93.9 (+11.5%)

Table 2: Comparing the performance of different LLMs as backbones for LLM-based methods in terms of average **AUROC (%)** on 13 classification datasets, evaluated using MLP and XGBoost as the downstream tabular learning models, respectively. All results are averaged over 5 runs.

Model	MLP						XGBoost					
	OpenFE	AutoGluon	CAAFE	OCTree	Ours (w/o)	Ours (w/ human)	OpenFE	AutoGluon	CAAFE	OCTree	Ours (w/o)	Ours (w/ human)
Deepseek-v3	83.5	83.5	84.9	85.5	86.1	86.4	85.6	85.4	86.6	87.3	88.2	88.6
GPT-3.5-turbo	83.5	83.5	83.2	84.2	84.6	85.1	85.6	85.4	85.2	86.0	86.5	87.1
GPT-4o	83.5	83.5	84.3	84.7	85.3	85.5	85.6	85.4	85.9	86.7	87.4	87.4
GPT-5	83.5	83.5	85.5	85.8	85.9	86.5	85.6	85.4	87.1	87.7	88.0	88.7

information on how to construct successful features for these widely used datasets, we additionally include a proprietary company dataset of predicting users’ conversion intentions, which cannot be accessed by the LLM, to provide a more robust evaluation. Detailed information about each dataset is provided in Appendix C.1.

Baselines and Operationalizing the Proposed Method. We consider both AutoML and LLM-based feature engineering methods as baselines. For AutoML methods, we include OpenFE (Zhang et al., 2023) and AutoGluon (Erickson et al., 2020). For LLM-based methods, we consider CAAFE(Hollmann et al., 2023) and OCTree(Nam et al., 2024a). To evaluate the effectiveness of feature engineering, we employ MLP (Rumelhart et al., 1986) and XGBoost (Chen & Guestrin, 2016) as downstream prediction models. For non-LLM methods, the feature engineering process proceeds until convergence to their best performance. For all LLM-based methods, we use GPT-4o (OpenAI, 2024) as the backbone model to generate feature operations in each round with a sampling temperature of 1, and the maximum iteration budget is set at 50. For the proposed method, the LLM generates 15 candidate feature transformation operations per prompt in each iteration. We specifically evaluate our method under two settings: one where the human collaborator is absent (*w/o Human*), and one where the human collaborator is available (*w/ Human*). To simulate the *w/ Human* setting, we employ GPT-4o as a proxy as the human expert to provide the preference feedback. In particular, for each dataset, we first fit a base classifier and use SHAP (Lundberg & Lee, 2017) to identify the most important features for the task. These feature importance scores are then converted into the expert prompts, enabling the proxy model to judge which feature pairs are more promising. Each dataset is randomly partitioned into 80% training and 20% validation sets, and this process is repeated for 5 iterations to evaluate each method’s performance. For detailed prompt template used in each round, please see Appendix D.

4.2 EVALUATION RESULTS

Table 1 presents the comparison of final feature engineering performance across 13 classification datasets using the proposed method, LLM-based baselines, and AutoML baselines with GPT-4o model as the backbone to generate feature operations for all LLM-based methods. Overall, we observe that both *Ours (w/o human)* and *Ours (w/ human)* consistently outperform the best baseline methods across different datasets. Specifically, when using MLP as the evaluation model, *Ours (w/o human)* achieves an average error rate reduction of 7.24%, while *Ours (w/ human)* achieves 8.96% compared to the best baseline. Similarly, when using the XGBoost as the evaluator, *Ours (w/o human)* achieves 9.02%, and *Ours (w/ human)* achieves 11.23% average error rate reduction over the best baselines. Below, we summarized key observations.

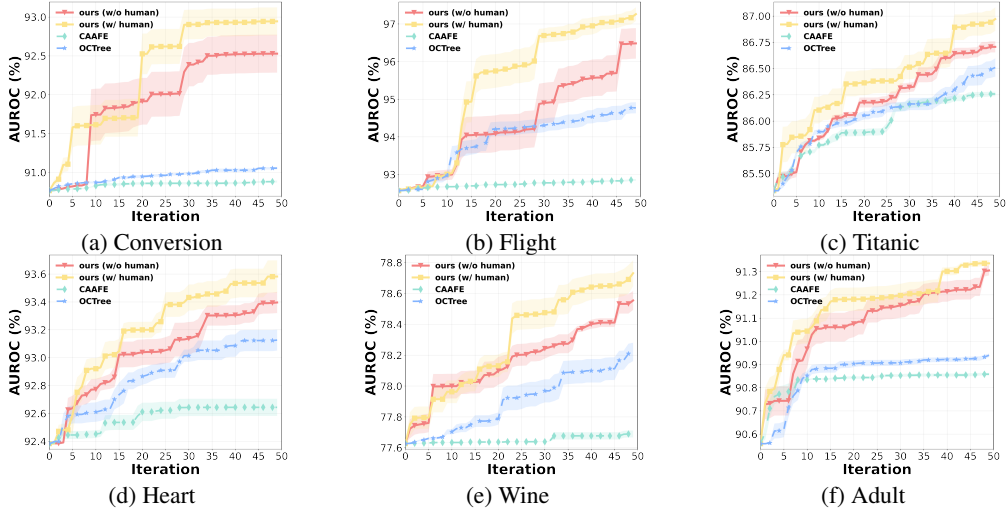


Figure 1: Comparing the performance trajectories of the proposed method with two LLM-based baselines (CAAFE and OCTree) in the feature engineering process, using an iteration budget of 50 and MLP as the tabular learner across six tasks. Error shade indicates the standard error of the mean.

LLM-based feature engineering methods outperform traditional non-LLM automatic feature engineering approaches. We found that feature engineering methods leveraging large language models (e.g., CAAFE, OCTree, and our proposed method) generally outperform traditional automatic feature engineering methods such as OpenFE and AutoGluon. We attribute this improvement to the strong semantic understanding, reasoning, and generative capabilities of LLMs, which enable them to efficiently generate effective feature transformation operations tailored to different tasks.

Explicitly modeling utility and uncertainty of feature operations improves LLM-powered feature engineering. Unlike prior LLM-based methods such as CAAFE and OCTree, our proposed approach generally leads to improved performance across different tasks. As a proof of concept, on the proprietary company-owned *conversion dataset*, OCTree achieves an AUROC of 91.1%. In contrast, *Ours (w/o human)* achieves 92.4% and *Ours (w/ human)* achieves 92.6% further under the same iteration budget as OCTree.

Incorporating human preference feedback improves performance. Finally, we evaluated the impact of incorporating human preference feedback on the performance of our proposed feature engineering method. We observed that the addition of human feedback consistently improves the method’s performance across most tasks compared to when no feedback is available. Specifically, in the MLP model, the incorporation of human feedback increases the average error reduction rate by 1.72% compared to the best baseline. Similarly, in the XGBoost model, the improvement increases further to 3.21% of the average error reduction. For the remaining regression tasks, we observe similar performance trends across both baseline methods and our proposed method (see Appendix C.2).

In addition to using GPT-4o as the backbone model, we further compare the performance of all LLM-based feature engineering methods under alternative backbone generators. For the *Ours (w/ human)*, we continue to use GPT-4o to simulate human preference feedback to ensure consistency across different backbone settings. As shown in Table 2, we evaluate four LLMs—DeepSeek-V3 (Liu et al., 2024), GPT-3.5-Turbo (Ouyang et al., 2022), GPT-4o (OpenAI, 2024), and GPT-5 (OpenAI, 2025) across the same 13 datasets using both MLP and XGBoost as downstream tabular models. Across all backbones, both *Ours (w/o human)* and *Ours (w/ human)* consistently outperform LLM-based and non-LLM baselines, demonstrating that the proposed framework is robust to the choice of backbone model. Even with a weaker generator such as GPT-3.5-Turbo, our method can still maintain strong performance.

4.3 ANALYSIS OF ITERATIVE GAINS IN FEATURE ENGINEERING

To better understand the advantage of our approach over LLM-based baselines that are based solely on LLM’s internal heuristics to generate and select feature operations, we analyze iterative gains throughout the feature engineering process by comparing the performance trajectories of our method (*w/o human* and *w/ human*) against LLM-based baselines. Figures 1a to Figure 1f present the performance trajectories of our method versus CAAFE and OCTree during the feature engineering

Table 3: Runtime breakdown of the proposed feature engineering pipelines when varying the number of initial features from 10 to 10,000 with a full dataset of 10,000 instances.

Features	LLM (s)	Surrogate (s)	UCB (s)	Eval (s)
10	1.82	0.17	0.006	1.79
50	1.82	0.16	0.005	1.24
100	1.82	0.19	0.005	1.78
1,000	1.82	0.20	0.009	8.4
10,000	1.82	0.57	0.018	23.4

Table 4: Runtime breakdown of the proposed feature engineering pipeline when varying the number of training instances from 1,000 to 100,000 with 100 initial feature columns.

Samples	LLM (s)	Surrogate (s)	UCB (s)	Eval (s)
1,000	1.82	0.17	0.005	0.28
5,000	1.82	0.18	0.005	0.89
10,000	1.82	0.23	0.006	1.47
50,000	1.82	0.18	0.006	5.22
100,000	1.82	0.18	0.005	10.65

process, under an iteration budget of 50, using MLP as the tabular learner. Visually, we observe that unlike CAAFE and OCTree, which often become trapped in local optima or experience performance stagnation, our method is able to identify high-impact feature operations that lead to notable performance jumps at various points and make steady progress during the iteration process. Furthermore, when investigating the impact of incorporating the selectively elicited human feedback, we observe that it often helps the algorithm redirect the feature search toward more promising operations, which enables the algorithm to make sharper gains and achieve even higher performance compared to the setting without human input. Similar trends are observed in other datasets (see Appendix C.3).

4.4 ANALYSIS OF COMPUTATIONAL SCALABILITY OF THE PROPOSED METHOD

To understand the computational scalability of the proposed method, we measured the runtime of each component of the LLM-powered feature engineering pipeline within a single iteration, which consists of four steps:

1. calling the LLM to generate candidate feature transformations.
2. fitting the BNN surrogate model using the accumulated observations.
3. computing UCB scores for the proposed candidates.
4. evaluating the selected transformation using the downstream tabular model.

Here, steps 2 and 3 are the specific computational components of our framework, while steps 1 and 4 are shared across all LLM-based pipelines. We then conducted controlled experiments on synthetic binary-classification datasets by systematically varying the number of initial feature columns and the number of data instances to directly measure how each component of the pipeline scales under datasets of different sizes. All feature columns were sampled from standard normal distributions, labels from a Bernoulli distribution, and an MLP was used as the downstream evaluator. All LLM calls were made using GPT-4o, and for the downstream evaluation step, we fixed the MLP training to a single epoch to ensure consistent and comparable timing across all conditions. We first fixed the dataset size to 10,000 instances and varied the number of initial features from 10 to 10,000. As shown in Table 3, the time required for fitting surrogate model and UCB score computation increases only mildly with feature dimensionality, whereas the downstream evaluator dominates the runtime as the number of initial features grows. For instance, with 10,000 initial features, the surrogate model and UCB steps together account for only about 2.2% of the total runtime. Next, we fixed the number of initial features to 100 and varied the dataset size from 1,000 to 100,000 rows. As shown in Table 4, the surrogate fitting and UCB computation times remain nearly constant across all sample sizes and contribute only a small percentage of the total runtime, because both operate at the feature-operation level and are independent of the number of data instances. In contrast, the downstream evaluation time increases with dataset size, as it requires training the MLP on the full dataset. Overall, these results indicate that our method scales favorably with both feature dimensionality and dataset size.

4.5 USER STUDY: HOW DO HUMANS PERFORM AND PERCEIVE WITH OUR METHOD?

Finally, to understand how actual users would collaborate with our algorithm to complete the feature engineering task, we conducted a user study, where we selected the flight dataset of predicting passengers’ satisfaction levels as the feature engineering task. We designed three treatments by varying the ways in which participants could collaborate with the LLM to complete the task:

- **CONTROL:** The human fully leads the feature engineering process. In each round, the human needs to provide language instructions about what to do, and the LLM will parse the instructions to create the feature operations.
- **SELF REASONING (SR):** In this treatment, the overall algorithm remains the same as our proposed method, except that the querying mechanism is modified so the LLM autonomously de-

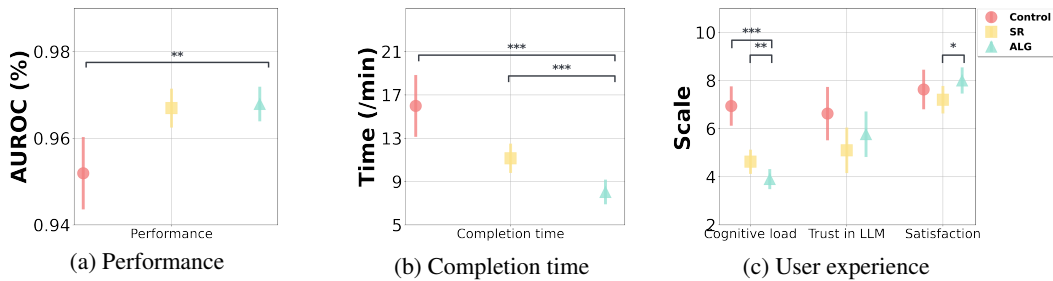


Figure 2: Comparing participants’ *average* final feature engineering performance, completion time, and the user experience perceptions for the flight satisfaction prediction task in the CONTROL, SR, and our ALG treatment, respectively. Error bars represent the 95% confidence intervals of the mean values. *, **, and *** denote statistical significance levels of 0.1, 0.05, and 0.01 respectively.

cides in each round whether to query human preference feedback, rather than being triggered by our algorithm.

- OURS (ALG): In this treatment, the human preference feedback is triggered by our proposed method.

We recruited 31 machine learning engineers/researchers or graduate students with a background in AI/ML as participants⁷. Each participant was randomly assigned to one of the three treatments. At the beginning of the study, participants were provided with SHAP-generated explanations, which highlighted the importance of each original feature in the dataset, to equip them with task-specific expertise. Following this, participants proceeded with the feature engineering task in different ways of collaborating with the LLM depending on the assigned treatment until the iteration budget was exhausted. We used GPT-4o as the backbone model to generate feature transformation operations and MLP as the tabular learner to evaluate the utility of the feature operations, with the iteration budget of feature engineering process set to 40 for all treatments. Finally, participants were required to complete an exit survey to report their perceptions on the overall feature engineering process. In this survey, we used the NASA Task Load Index (Hart & Staveland, 1988) to measure the cognitive load experienced by participants during the feature engineering process, including their perceived mental demand, time pressure, effort level, and frustration. In addition, participants were also asked to rate the overall satisfaction, and the trust in using the system for future on a scale from 1 to 10.

Figure 2a compares the participants’ average final feature engineering performance across three treatments. One-way ANOVA and subsequent Tukey’s HSD test show that participants who worked under our ALG framework demonstrated significantly higher final feature engineering task performance compared to those in the CONTROL treatment ($p = 0.011$). Figure 2b compares participants’ average task completion time across the three treatments. Visually, we observe that participants in our ALG framework exhibited higher time efficiency compared to the other two conditions. One-way ANOVA and further Tukey’s HSD test show that participants under our ALG framework had significantly lower completion times compared to those in CONTROL ($p < 0.001$) and those in SR ($p = 0.02$). We finally move on to investigate how participants perceive their experience under different treatments. As shown in Figure 2c, participants in our ALG framework reported significantly lower cognitive load compared to those in CONTROL ($p < 0.001$) and those in SR ($p = 0.043$), as well as a marginally significantly higher satisfaction compared to those in SR ($p = 0.072$).

5 CONCLUSION

In this paper, we propose a human–LLM collaborative feature engineering framework for tabular learning. We begin by decoupling the transformation operation proposal and selection processes, where LLMs are used solely to generate operation candidates, while the selection is guided by explicitly modeling the utility and uncertainty of each proposed operation. We then design a mechanism within the framework that selectively elicits and incorporates human expert preference feedback into the selection process to help identify more effective operations to explore. Our evaluations on the both synthetic study and real user study demonstrate that the proposed framework improves feature engineering performance across a variety of tabular datasets and reduces users’ cognitive load during the feature engineering process.

⁷This study was approved by the author’s Institutional Review Board.

REFERENCES

Nikhil Abhyankar, Parshin Shojaee, and Chandan K Reddy. Llm-fe: Automated feature engineering for tabular data with llms as evolutionary optimizers. *arXiv preprint arXiv:2503.14434*, 2025.

Josh Achiam, Steven Adler, Sandhini Agarwal, Lama Ahmad, Ilge Akkaya, Florencia Leoni Aleman, Diogo Almeida, Janko Altenschmidt, Sam Altman, Shyamal Anadkat, et al. Gpt-4 technical report. *arXiv preprint arXiv:2303.08774*, 2023.

Yousef H Alfaifi. Recommender systems applications: Data sources, features, and challenges. *Information*, 15(10):660, 2024.

Rohan Alur, Manish Raghavan, and Devavrat Shah. Human expertise in algorithmic prediction. *Advances in Neural Information Processing Systems*, 37:138088–138129, 2024.

Peter Auer, Nicolò Cesa-Bianchi, and Paul Fischer. Finite-time analysis of the multiarmed bandit problem. *Machine Learning*, 47(2-3):235–256, 2002. doi: 10.1023/A:1013689704352.

Arun Kumar AV, Santu Rana, Alistair Shilton, and Svetha Venkatesh. Human-ai collaborative bayesian optimisation. *Advances in neural information processing systems*, 35:16233–16245, 2022.

Gagan Bansal, Besmira Nushi, Ece Kamar, Walter S Lasecki, Daniel S Weld, and Eric Horvitz. Beyond accuracy: The role of mental models in human-ai team performance. In *Proceedings of the AAAI conference on human computation and crowdsourcing*, volume 7, pp. 2–11, 2019a.

Gagan Bansal, Besmira Nushi, Ece Kamar, Daniel S Weld, Walter S Lasecki, and Eric Horvitz. Updates in human-ai teams: Understanding and addressing the performance/compatibility trade-off. In *Proceedings of the AAAI conference on artificial intelligence*, volume 33, pp. 2429–2437, 2019b.

Sebastian Bordt, Harsha Nori, Vanessa Rodrigues, Besmira Nushi, and Rich Caruana. Elephants never forget: Memorization and learning of tabular data in large language models. *arXiv preprint arXiv:2404.06209*, 2024.

Mohamed Bouadi, Arta Alavi, Salima Benberou, and Mourad Ouziri. Synergizing large language models and knowledge-based reasoning for interpretable feature engineering. In *Proceedings of the ACM on Web Conference 2025*, pp. 2606–2620, 2025.

Stephen P Boyd and Lieven Vandenberghe. *Convex optimization*. Cambridge university press, 2004.

Zana Buçinca, Maja Barbara Malaya, and Krzysztof Z Gajos. To trust or to think: cognitive forcing functions can reduce overreliance on ai in ai-assisted decision-making. In *Proceedings of the ACM on Human-Computer Interaction*, 5(CSCW1):1–21, 2021.

Tianqi Chen and Carlos Guestrin. XGBoost: A scalable tree boosting system. In *Proceedings of the 22nd ACM SIGKDD International Conference on Knowledge Discovery and Data Mining*, pp. 785–794. ACM, 2016. doi: 10.1145/2939672.2939785.

Chun-Wei Chiang, Zhuoran Lu, Zhuoyan Li, and Ming Yin. Are two heads better than one in ai-assisted decision making? comparing the behavior and performance of groups and individuals in human-ai collaborative recidivism risk assessment. In *Proceedings of the 2023 CHI Conference on Human Factors in Computing Systems*, pp. 1–18, 2023.

Chun-Wei Chiang, Zhuoran Lu, Zhuoyan Li, and Ming Yin. Enhancing ai-assisted group decision making through llm-powered devil’s advocate. In *Proceedings of the 29th International Conference on Intelligent User Interfaces*, pp. 103–119, 2024.

Giovanni De Toni, Nastaran Okati, Suhas Thejaswi, Eleni Straitouri, and Manuel Rodriguez. Towards human-ai complementarity with prediction sets. *Advances in Neural Information Processing Systems*, 37:31380–31409, 2024.

Tuan Dinh, Yuchen Zeng, Ruisu Zhang, Ziqian Lin, Michael Gira, Shashank Rajput, Jy-yong Sohn, Dimitris Papailiopoulos, and Kangwook Lee. Lift: Language-interfaced fine-tuning for non-language machine learning tasks. *Advances in Neural Information Processing Systems*, 35:11763–11784, 2022.

Nick Erickson, Jonas Mueller, Alexander Shirkov, Hang Zhang, Pedro Larroy, Mu Li, and Alexander Smola. Autogluon-tabular: Robust and accurate automl for structured data. *arXiv preprint arXiv:2003.06505*, 2020.

Sungwon Han, Jinsung Yoon, Sercan O Arik, and Tomas Pfister. Large language models can automatically engineer features for few-shot tabular learning. *arXiv preprint arXiv:2404.09491*, 2024.

Sungwon Han, Sungkyu Park, and Seungeon Lee. Tabular feature discovery with reasoning type exploration. *arXiv preprint arXiv:2506.20357*, 2025.

Sandra G Hart and Lowell E Staveland. Development of nasa-tlx (task load index): Results of empirical and theoretical research. In *Advances in psychology*, volume 52, pp. 139–183. Elsevier, 1988.

Stefan Heggelmann, Alejandro Buendia, Hunter Lang, Monica Agrawal, Xiaoyi Jiang, and David Sontag. Tabllm: Few-shot classification of tabular data with large language models. In *International conference on artificial intelligence and statistics*, pp. 5549–5581. PMLR, 2023.

Noah Hollmann, Samuel Müller, and Frank Hutter. Large language models for automated data science: Introducing caafe for context-aware automated feature engineering. *Advances in Neural Information Processing Systems*, 36:44753–44775, 2023.

Carl Hvarfner, Danny Stoll, Artur Souza, Marius Lindauer, Frank Hutter, and Luigi Nardi. pi-bo: Augmenting acquisition functions with user beliefs for bayesian optimization. *arXiv preprint arXiv:2204.11051*, 2022.

Daniel Kahneman and Amos Tversky. Prospect theory: An analysis of decision under risk. In *Handbook of the fundamentals of financial decision making: Part I*, pp. 99–127. World Scientific, 2013.

Jeonghyun Ko, Gyeongyun Park, Donghoon Lee, and Kyunam Lee. Ferg-ilm: Feature engineering by reason generation large language models. *arXiv preprint arXiv:2503.23371*, 2025.

Vivian Lai, Chacha Chen, Q Vera Liao, Alison Smith-Renner, and Chenhao Tan. Towards a science of human-ai decision making: a survey of empirical studies. *arXiv preprint arXiv:2112.11471*, 2021.

Yucen Lily Li, Tim GJ Rudner, and Andrew Gordon Wilson. A study of bayesian neural network surrogates for bayesian optimization. *arXiv preprint arXiv:2305.20028*, 2023a.

Zhuoyan Li and Ming Yin. Utilizing human behavior modeling to manipulate explanations in ai-assisted decision making: the good, the bad, and the scary. *Advances in Neural Information Processing Systems*, 37:5025–5047, 2024.

Zhuoyan Li, Zhuoran Lu, and Ming Yin. Modeling human trust and reliance in ai-assisted decision making: A markovian approach. In *Proceedings of the AAAI Conference on Artificial Intelligence*, volume 37, pp. 6056–6064, 2023b.

Zhuoyan Li, Zhuoran Lu, and Ming Yin. Decoding ai’s nudge: A unified framework to predict human behavior in ai-assisted decision making. In *Proceedings of the AAAI Conference on Artificial Intelligence*, volume 38, pp. 10083–10091, 2024.

Zhuoyan Li, Hangxiao Zhu, Zhuoran Lu, Ziang Xiao, and Ming Yin. From text to trust: Empowering ai-assisted decision making with adaptive llm-powered analysis. In *Proceedings of the 2025 CHI Conference on Human Factors in Computing Systems*, pp. 1–18, 2025.

Aixin Liu, Bei Feng, Bing Xue, Bingxuan Wang, Bochao Wu, Chengda Lu, Chenggang Zhao, Chengqi Deng, Chenyu Zhang, Chong Ruan, et al. Deepseek-v3 technical report. *arXiv preprint arXiv:2412.19437*, 2024.

Zhuoran Lu, Zhuoyan Li, Chun-Wei Chiang, and Ming Yin. Strategic adversarial attacks in ai-assisted decision making to reduce human trust and reliance. In *IJCAI*, pp. 3020–3028, 2023.

Scott M Lundberg and Su-In Lee. A unified approach to interpreting model predictions. *Advances in neural information processing systems*, 30, 2017.

Syed Hasan Amin Mahmood, Zhuoran Lu, and Ming Yin. Designing behavior-aware ai to improve the human-ai team performance in ai-assisted decision making. International Joint Conferences on Artificial Intelligence Organization, 2024.

Hussein Mozannar, Jimin Lee, Dennis Wei, Prasanna Sattigeri, Subhro Das, and David Sontag. Effective human-ai teams via learned natural language rules and onboarding. *Advances in neural information processing systems*, 36:30466–30498, 2023.

Jaehyun Nam, Jihoon Tack, Kyungmin Lee, Hankook Lee, and Jinwoo Shin. Stunt: Few-shot tabular learning with self-generated tasks from unlabeled tables. *arXiv preprint arXiv:2303.00918*, 2023.

Jaehyun Nam, Kyuyoung Kim, Seunghyuk Oh, Jihoon Tack, Jaehyung Kim, and Jinwoo Shin. Optimized feature generation for tabular data via llms with decision tree reasoning. *Advances in Neural Information Processing Systems*, 37:92352–92380, 2024a.

Jaehyun Nam, Woomin Song, Seong Hyeon Park, Jihoon Tack, Sukmin Yun, Jaehyung Kim, Kyu Hwan Oh, and Jinwoo Shin. Tabular transfer learning via prompting llms. *arXiv preprint arXiv:2408.11063*, 2024b.

OpenAI. GPT-4o system card. arXiv:2410.21276, 2024. URL <https://arxiv.org/abs/2410.21276>.

OpenAI. Gpt-5 system overview, 2025. OpenAI Model Documentation.

Long Ouyang et al. Training language models to follow instructions with human feedback. *arXiv preprint arXiv:2203.02155*, 2022.

Paul Resnick and Hal R Varian. Recommender systems. *Communications of the ACM*, 40(3):56–58, 1997.

David E. Rumelhart, Geoffrey E. Hinton, and Ronald J. Williams. Learning representations by back-propagating errors. *Nature*, 323(6088):533–536, 1986. doi: 10.1038/323533a0.

Jasper Snoek, Hugo Larochelle, and Ryan P Adams. Practical bayesian optimization of machine learning algorithms. *Advances in neural information processing systems*, 25, 2012.

Jasper Snoek, Oren Rippel, Kevin Swersky, Ryan Kiros, Nadathur Satish, Narayanan Sundaram, Mostofa Patwary, Mr Prabhat, and Ryan Adams. Scalable bayesian optimization using deep neural networks. In *International conference on machine learning*, pp. 2171–2180. PMLR, 2015.

Artur Souza, Luigi Nardi, Leonardo B Oliveira, Kunle Olukotun, Marius Lindauer, and Frank Hutter. Bayesian optimization with a prior for the optimum. In *Joint European Conference on Machine Learning and Knowledge Discovery in Databases*, pp. 265–296. Springer, 2021.

Kailas Vodrahalli, Tobias Gerstenberg, and James Y Zou. Uncalibrated models can improve human-ai collaboration. *Advances in Neural Information Processing Systems*, 35:4004–4016, 2022.

Dakuo Wang, Justin D Weisz, Michael Muller, Parikshit Ram, Werner Geyer, Casey Dugan, Yla Tausczik, Horst Samulowitz, and Alexander Gray. Human-ai collaboration in data science: Exploring data scientists’ perceptions of automated ai. *Proceedings of the ACM on human-computer interaction*, 3(CSCW):1–24, 2019.

Zi Wang, George E Dahl, Kevin Swersky, Chansoo Lee, Zachary Nado, Justin Gilmer, Jasper Snoek, and Zoubin Ghahramani. Pre-trained gaussian processes for bayesian optimization. *Journal of Machine Learning Research*, 25(212):1–83, 2024.

Zifeng Wang, Chufan Gao, Cao Xiao, and Jimeng Sun. Anypredict: Foundation model for tabular prediction. *CoRR*, 2023.

Zixi Wei, Yuzhou Cao, and Lei Feng. Exploiting human-ai dependence for learning to defer. In *Forty-first International Conference on Machine Learning*, 2024.

Wenjie Xu, Masaki Adachi, Colin Jones, and Michael A Osborne. Principled bayesian optimization in collaboration with human experts. *Advances in Neural Information Processing Systems*, 37: 104091–104137, 2024a.

Wenjie Xu, Wenbin Wang, Yuning Jiang, Bratislav Svetozarevic, and Colin N Jones. Principled preferential bayesian optimization. *arXiv preprint arXiv:2402.05367*, 2024b.

Zhitong Xu, Haitao Wang, Jeff M Phillips, and Shandian Zhe. Standard gaussian process is all you need for high-dimensional bayesian optimization. *arXiv preprint arXiv:2402.02746*, 2024c.

Jiahuan Yan, Bo Zheng, Hongxia Xu, Yiheng Zhu, Danny Z Chen, Jimeng Sun, Jian Wu, and Jintai Chen. Making pre-trained language models great on tabular prediction. *arXiv preprint arXiv:2403.01841*, 2024.

Chengdong Yang, Hongrui Liu, Daixin Wang, Zhiqiang Zhang, Cheng Yang, and Chuan Shi. Flag: Fraud detection with llm-enhanced graph neural network. In *Proceedings of the 31st ACM SIGKDD Conference on Knowledge Discovery and Data Mining V.2*, KDD '25, pp. 5150–5160, New York, NY, USA, 2025. Association for Computing Machinery. ISBN 9798400714542. doi: 10.1145/3711896.3737220. URL <https://doi.org/10.1145/3711896.3737220>.

Tianping Zhang, Zheyu Zhang, Zhiyuan Fan, Haoyan Luo, Fengyuan Liu, Qian Liu, Wei Cao, and Jian Li. Openfe: Automated feature generation with expert-level performance. In *Proceedings of the 40th International Conference on Machine Learning*, volume 202 of *Proceedings of Machine Learning Research*, pp. 41880–41901. PMLR, 2023. URL <https://proceedings.mlr.press/v202/zhang23ay.html>.

Yanlin Zhang, Ning Li, Quan Gan, Weinan Zhang, David Wipf, and Minjie Wang. Elf-gym: Evaluating large language models generated features for tabular prediction. In *Proceedings of the 33rd ACM International Conference on Information and Knowledge Management*, pp. 5420–5424, 2024.

A PROOF FOR TECHNICAL LEMMAS IN SECTION 3

A.1 COMPLETE PROOF FOR LEMMA 3.1

Given the surrogate model posterior distribution $q_t(\boldsymbol{\theta}) = \mathcal{N}(\boldsymbol{\theta}; \mathbf{M}_t, \boldsymbol{\Sigma}_t)$, and the surrogate model $\hat{g}(\phi(e); \boldsymbol{\theta})$, we first perform a first-order Taylor expansion of $\hat{g}(\phi(e); \boldsymbol{\theta})$ around \mathbf{M}_t :

$$\begin{aligned}\hat{g}(\phi(e); \boldsymbol{\theta}) &= \underbrace{\hat{g}(\phi(e); \mathbf{M}_t)}_{=: c_t(e)} + \underbrace{\nabla_{\boldsymbol{\theta}} \hat{g}(\phi(e); \mathbf{M}_t) (\boldsymbol{\theta} - \mathbf{M}_t)}_{=: \phi_t(e)^\top} + \underbrace{R_2(e; \boldsymbol{\theta})}_{=: \mathbf{w}} \\ &= c_t(e) + \phi_t(e)^\top \mathbf{w} + R_2(e; \boldsymbol{\theta})\end{aligned}$$

where $\mathbf{w} \sim \mathcal{N}(\mathbf{w}; 0, \boldsymbol{\Sigma}_t)$. Since our surrogate model \hat{g} is implemented as a multilayer perceptron (MLP) with 1-Lipschitz activations (e.g., ReLU), based on the prior research (Boyd & Vandenberghe, 2004), this indicates that the second-order remainder $R_2(e; \boldsymbol{\theta})$ is locally bounded as $|R_2(e; \boldsymbol{\theta})| \leq C \|\mathbf{w}\|_2^2$ where C is model architecture-dependent constant. We therefore omit R_2 and use the *linearized surrogate model* in the subsequent proof:

$$\hat{g}_{\text{lin}}(\phi(e); \mathbf{w}) = c_t(e) + \phi_t(e)^\top \mathbf{w}, \quad \text{where } \mathbf{w} \sim \mathcal{N}(\mathbf{w}; 0, \boldsymbol{\Sigma}_t)$$

Assumption A.1 (Utility Linearity). *Given some model weights $\mathbf{w}^* \sim \mathcal{N}(\mathbf{0}, \boldsymbol{\Sigma}_t)$, the true utility of a feature transformation operation $g(e)$ can be linearly represented in the feature space $\phi(\cdot)$, i.e., $g(e) = c_t(e) + \phi_t(e)^\top \mathbf{w}^*$.*

Lemma A.1. *By Assumption A.1, the standardized deviation $\Psi = \frac{g(e) - \mu_t(e)}{\sigma_t(e)}$ is 1-sub-Gaussian, i.e., $\mathbb{E}[\exp(\lambda\Psi)] \leq \exp\left(\frac{\lambda^2}{2}\right)$, $\forall \lambda \in \mathbb{R}$.*

Proof. Given the predicted *expected utility* $\mu_t(e)$ of a candidate operation e and its corresponding *uncertainty* $\sigma_t^2(e)$:

$$\mu_t(e) = \mathbb{E}_{q_t(\boldsymbol{\theta})}[\hat{g}(\phi(e); \boldsymbol{\theta})], \quad \sigma_t^2(e) = \mathbb{E}_{q_t(\boldsymbol{\theta})}[\hat{g}(\phi(e); \boldsymbol{\theta})^2] - \mu_t(e)^2$$

As the surrogate model $\hat{g}(\cdot)$ can be approximated as the linearized surrogate model $\hat{g}_{\text{lin}}(\cdot)$, the expected utility $\mu_t(e)$ and the uncertainty $\sigma_t^2(e)$ can be represented as:

$$\mu_t(e) = \mathbb{E}[c_t(e) + \phi_t(e)^\top \mathbf{w}] = c_t(e), \quad \sigma_t^2(e) = \text{Var}(c_t(e) + \phi_t(e)^\top \mathbf{w}) = \phi_t(e)^\top \boldsymbol{\Sigma}_t \phi_t(e)$$

Consequently, the standard deviation Ψ is:

$$\Psi = \frac{g(e) - \mu_t(e)}{\sigma_t(e)} = \frac{c_t(e) + \phi_t(e)^\top \mathbf{w}^* - c_t(e)}{\sqrt{\phi_t(e)^\top \boldsymbol{\Sigma}_t \phi_t(e)}} = \frac{\phi_t(e)^\top \mathbf{w}^*}{\sqrt{\phi_t(e)^\top \boldsymbol{\Sigma}_t \phi_t(e)}}$$

Since $\mathbf{w}^* \sim \mathcal{N}(0, \boldsymbol{\Sigma}_t)$, we have $\phi_t(e)^\top \mathbf{w}^* \sim \mathcal{N}(0, \phi_t(e)^\top \boldsymbol{\Sigma}_t \phi_t(e))$. Thus, $\Psi = \frac{\phi_t(e)^\top \mathbf{w}^*}{\sqrt{\phi_t(e)^\top \boldsymbol{\Sigma}_t \phi_t(e)}} \sim \mathcal{N}(0, 1)$, and $\mathbb{E}[\exp(\lambda\Psi)] \leq \exp\left(\frac{\lambda^2}{2}\right)$.

Lemma 3.1 *At round t , the LLM M proposes a set of candidate operations \mathcal{S}_t . For any $\delta \in (0, 1)$, with probability at least $1 - \delta$, the deviation between the actual utility $g(e)$ and the predicted expected utility $\mu_t(e)$ is uniformly bounded for all $e \in \mathcal{S}_t$:*

$$\mathbb{P}\left(\forall t \geq 1, \forall e \in \mathcal{S}_t : |g(e) - \mu_t(e)| \leq \sqrt{\beta_t} \sigma_t(e)\right) \geq 1 - \delta, \quad \beta_t = 2 \log\left(\frac{|\mathcal{S}_t| \pi^2 t^2}{3\delta}\right)$$

Proof. By Lemma A.1, for any $u > 0$, we have:

$$\mathbb{P}(|g(e) - \mu_t(e)| > u \sigma_t(e)) = \mathbb{P}(|\Psi| > u) = 2\Phi(-u) \leq 2e^{-u^2/2}$$

where Φ is the standard normal CDF. At round t , given the LLM-proposed feature set \mathcal{S}_t , setting $u = \sqrt{\beta_t}$ and applying the union bound yields:

$$\mathbb{P}\left(\exists e \in \mathcal{S}_t : |g(e) - \mu_t(e)| > \sqrt{\beta_t} \sigma_t(e)\right) \leq \sum_{e \in \mathcal{S}_t} 2e^{-\beta_t/2} = 2|\mathcal{S}_t| e^{-\beta_t/2}$$

Let

$$\beta_t = 2 \log \left(\frac{|\mathcal{S}_t| \pi^2 t^2}{3\delta} \right)$$

Then

$$\mathbb{P} \left(\exists e \in \mathcal{S}_t : |g(e) - \mu_t(e)| > \sqrt{\beta_t} \sigma_t(e) \right) \leq \frac{6\delta}{\pi^2 t^2}$$

Define the failure event at round t :

$$\mathcal{F}_t := \left\{ \exists e \in \mathcal{S}_t : |g(e) - \mu_t(e)| > \sqrt{\beta_t} \sigma_t(e) \right\}$$

Apply the union bound over all rounds $t \geq 1$, we have:

$$\mathbb{P} \left(\bigcup_{t=1}^{\infty} \mathcal{F}_t \right) \leq \sum_{t=1}^{\infty} \mathbb{P}(\mathcal{F}_t) \leq \sum_{t=1}^{\infty} \frac{6\delta}{\pi^2 t^2} = \delta$$

Thus, with probability at least $1 - \delta$, the confidence bound holds uniformly for all $e \in \mathcal{S}_t$, $\forall t \geq 1$.

A.2 COMPLETE PROOF FOR LEMMA 3.2

Lemma 3.2 *By the Lemma 3.1, let $e_t^a \in \mathcal{S}_t$ be the UCB choice, the following holds for any operation $e_t^b \in \mathcal{S}_t \setminus \{e_t^a\}$ and $1 \leq t \leq T$:*

$$U(e_t^a, e_t^b; \kappa) = \mathbb{E}_{Z_t}[r'_t - r_t] \leq \max\{\text{UCB}_t(e_t^b) - \text{LCB}_t(e_t^a), 0\}$$

Proof. After receiving the human preference feedback Z_t , the posterior feature transformation operation is selected from the pair $\{e_t^a, e_t^b\}$. The regret reduction is defined as:

$$r_t - r'_t = [g(e_t^*) - g(e_t^a)] - [g(e_t^*) - g(e_t^b)] = g(e_t^b) - g(e_t^a),$$

where e_t^* is the optimal operation and $e_t' \in \{e_t^a, e_t^b\}$ is the final selected one. Since $e_t' \in \{e_t^a, e_t^b\}$, the regret reduction is bounded by:

$$r_t - r'_t \leq \max \{g(e_t^b) - g(e_t^a), 0\}.$$

Taking expectation over the preference feedback Z_t , we obtain:

$$U(e_t^a, e_t^b; \kappa) := \mathbb{E}_{Z_t}[r_t - r'_t] \leq \max \{g(e_t^b) - g(e_t^a), 0\}.$$

Under the confidence event in Lemma 3.1, for any $e \in \mathcal{S}_t$, the true utility is bounded as:

$$g(e) \in [\mu_t(e) - \sqrt{\beta_t} \sigma_t(e), \mu_t(e) + \sqrt{\beta_t} \sigma_t(e)],$$

i.e.,

$$g(e) \leq \text{UCB}_t(e) := \mu_t(e) + \sqrt{\beta_t} \sigma_t(e), \quad g(e) \geq \text{LCB}_t(e) := \mu_t(e) - \sqrt{\beta_t} \sigma_t(e).$$

Therefore,

$$g(e_t^b) - g(e_t^a) \leq \text{UCB}_t(e_t^b) - \text{LCB}_t(e_t^a),$$

and thus,

$$U(e_t^a, e_t^b; \kappa) \leq \max \{\text{UCB}_t(e_t^b) - \text{LCB}_t(e_t^a), 0\}.$$

B ALGORITHM

Algorithm 1 summarizes how does the proposed framework perform the iterative selection of LLM-proposed feature transformation operations in the feature engineering process.

C EVALUATIONS (ADDITIONAL DETAILS)

C.1 DESCRIPTIONS OF THE DATASETS USED IN THE MAIN STUDY

We evaluate our methods across 13 widely-used Kaggle classification datasets, covering diverse domains such as healthcare, finance, customer behavior, and public records. A brief description of each dataset is provided below:

Algorithm 1 Iterative Selection of LLM-Proposed Feature Transformation Operations

Input: Training Dataset $\mathcal{D}_{\text{train}}$, validation set $\mathcal{D}_{\text{eval}}$, LLM M , a tabular learner f , Iteration Budget T

- 1: Initialize $H_1 \leftarrow \emptyset$, the feature operation pool $S_0 \leftarrow \emptyset$
- 2: **for** $t = 1$ to T **do**
- 3: $S_t \leftarrow \{\text{feature operations proposed by } M \text{ in the round } t\} \cup S_{t-1} \setminus \{e_{t-1}^{\text{selected}}\}$
- 4: Fit the surrogate model $q_t(\theta)$ via equation 5
- 5: Select e_t^a via equation 8
- 6: **if** human expertise κ is not available **then**
- 7: $e_t^{\text{selected}} \leftarrow e_t^a$
- 8: **else**
- 9: Select e_t^b via equation 12
- 10: **if** the trigger conditions (equation 15) all hold **then**
- 11: Query human preference feedback: $Z_t \leftarrow \kappa(e_t^a, e_t^b)$
- 12: Update the surrogate model $q'_t(\theta)$ via equation 17
- 13: $e_t^{\text{selected}} \leftarrow \arg \max_{e \in \{e_t^a, e_t^b\}} \text{UCB}_t(e)$ via equation 18
- 14: **else**
- 15: $e_t^{\text{selected}} \leftarrow e_t^a$
- 16: Fit the tabular learner f on $\mathcal{D}_{\text{train}} \oplus e_t^{\text{selected}}$, and evaluate $g(e_t^{\text{selected}})$ on $\mathcal{D}_{\text{val}} \oplus e_t^{\text{selected}}$
- 17: $H_{t+1} \leftarrow H_t \cup \{(e_t^{\text{selected}}, g(e_t^{\text{selected}}))\}$
- 18: **if** $g(e_t^{\text{selected}}) > 0$ **then**
- 19: $\mathcal{D}_{\text{train}} \leftarrow \mathcal{D}_{\text{train}} \oplus e_t^{\text{selected}}$, $\mathcal{D}_{\text{eval}} \leftarrow \mathcal{D}_{\text{eval}} \oplus e_t^{\text{selected}}$
- 20: **return** $\{e_t^{\text{selected}}\}_{t=1}^T$, $\mathcal{D}_{\text{train}}$, and $\mathcal{D}_{\text{eval}}$

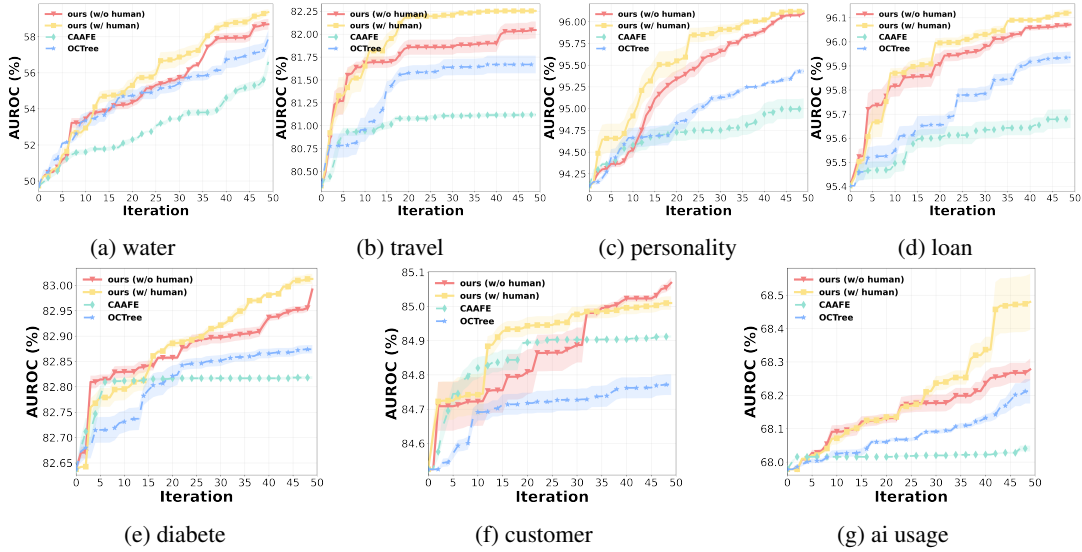


Figure C.1: Comparing the performance trajectories of the proposed method with two LLM-based baselines (CAAFE and OCTree) in the feature engineering process, using an iteration budget of 50 and MLP as the tabular learner across seven tasks. Error shade indicates the standard error of the mean.

C.2 EVALUATION RESULTS (ADDITIONAL DETAILS)

Table C.2 compares the performance of the proposed method, LLM-based baselines, and non-LLM-based baselines on 5 regression datasets in terms of error reduction rate (%) compared with the base learner with GPT-4o as the backbone model for all LLM-based methods, evaluated using MLP and XGBoost as the tabular learning models, respectively. We again observed that our proposed methods can outperform the baselines including AutoML methods and LLM-powered feature engineering approaches.

Dataset	Description	#Features	#Instances	Task Type
flight	Predict whether a flight is delayed based on schedule and airline attributes.	22	25,976	Classification
wine	Classify wine quality using physicochemical test results.	11	945	Classification
loan	Predict loan approval based on applicant demographic and financial attributes.	13	45,000	Classification
Diabetes	Diagnose diabetes from medical measurements of female patients.	21	40,000	Classification
titanic	Predict passenger survival on the Titanic from demographic and ticket info.	8	891	Classification
travel	Predict whether a customer purchased travel insurance or filed a claim.	8	63,326	Classification
ai_usage	Predict whether a survey respondent reports using AI tools.	8	10,000	Classification
water	Classify whether water is potable given physicochemical properties.	9	3,276	Classification
heart	Diagnose presence of heart disease based on clinical measurements.	11	918	Classification
adult	Predict if income exceeds \$50K based on census demographic data.	14	32,561	Classification
customer	Predict whether a telecom customer will churn from usage statistics.	20	7,043	Classification
personality	Predict Big Five personality types from survey responses.	7	2,900	Classification
conversion	Predict whether an online shopper will convert (make a purchase).	178	15,000	Classification
housing	Predict house price based on the information of the house.	9	20640	Regression
forest	Predict burned area in forest fires based on geographic information.	12	517	Regression
bike	Predict daily bike rental counts from weather and calendar info.	9	17,414	Regression
crab	Predict age of crabs based on biometric measurements.	8	3,893	Regression
insurance	Predict the insurance cost.	6	1,339	Regression

Table C.1: Summary of the datasets used in our experiments.

Table C.2: Comparing the performance of the proposed method, LLM-based baselines, and non-LLM-based baselines on 5 regression datasets in terms of normalized root mean square error with GPT-4o as the backbone model for all LLM-based methods, evaluated using MLP and XGBoost as the tabular learning models, respectively. The **best method** in each row is highlighted in **blue**, and the **best baseline method** is highlighted in **light blue**. The number in the brackets () indicate the error reduction rate compared to the **best baseline method**. All results are averaged over 5 runs.

Dataset	MLP						XGBoost					
	OpenFE	AutoGluon	CAAFE	OCTree	Ours (w/o human)	Ours (w/ human)	OpenFE	AutoGluon	CAAFE	OCTree	Ours (w/o human)	Ours (w/ human)
housing	0.316	0.319	0.292	0.283	0.270	0.266	0.228	0.231	0.224	0.221	0.216	0.214
forest	1.851	1.851	1.750	1.724	1.655	1.621	1.448	1.469	1.421	1.418	1.402	1.398
bike	0.295	0.302	0.282	0.274	0.262	0.261	0.216	0.219	0.211	0.208	0.203	0.201
crab	0.286	0.288	0.258	0.252	0.242	0.239	0.226	0.230	0.224	0.222	0.219	0.217
insurance	0.511	0.512	0.473	0.462	0.467	0.462	0.384	0.385	0.382	0.381	0.379	0.378

C.3 ANALYSIS OF ITERATIVE GAINS IN FEATURE ENGINEERING (ADDITIONAL DETAILS)

Figure C.1a to Figure C.1g compare the performance trajectories of the proposed method with two LLM-based baselines (CAAFE and OCTree) in the feature engineering process, using an iteration budget of 50 and MLP as the tabular learner across seven tasks.

D PROMPT TEMPLATE

The prompt for GPT-4o to propose feature transformation operations consists of two parts:

- **Introduction Prompt:**

You are an expert data scientist with deep expertise in feature engineering. You have the ability to:

- 1) Analyze patterns in previous feature performance to guide new feature creation
- 2) Reason about why certain features succeeded or failed
- 3) Design complementary features that address gaps in the current feature set
- 4) Consider domain knowledge and statistical relationships in your feature design

- **Instruction Prompt:**

Dataset Context:

- Task type: [CLASSIFICATION_OR_REGRESSION]
- Metric: [ROC_AUC_OR_OTHER]
- Columns (name:type): [COLS_WITH_TYPES]
- Target: <TARGET_NAME>
- Notes (missingness, skew, constraints): <DATA_NOTES>

Recent performance feedback: [PERFORMANCE HISTORY]

Remaining iteration budget: [BUDGET]

Strategic Reasoning

Based on the performance feedback above, consider:

1. What patterns do you see in the performance history?
2. What types of relationships might be missing from current features?
3. How can you build upon successful features while avoiding failed approaches?
4. What domain-specific insights can guide your next feature ideas ?

Task

Suggest up to K complementary NEW features** as a JSON list. Each item should include:

```
{
  "name": "snake_case_identifier",
  "explanation": "<detailed reasoning: why this feature helps, how it builds on feedback>",
  "reasoning": "<strategic thinking: what patterns from history inform this choice>",
  "code": "feature = <python expression using df[...] + helper ops>",
  "expected_benefit": "<specific hypothesis about how this will improve the model>"
}
```

Important Guidelines:

- Do not suggest features that need label information.
- Learn from rejected features - avoid similar patterns that failed
- Build upon successful features - create complementary variations
- You can try to combine multiple (N > 2) features to create a new feature to capture a more complex relationship.
- Ensure features are diverse and capture different aspects of the data
- Provide specific, actionable reasoning for each feature choice
- For the reasoning process and expected benefit analysis, be your best to be concise and clear.

Return ONLY the JSON list.

The prompt for GPT-4o to simulate as the human expert to provide the preference feedback consists of two parts:

- **Introduction Prompt:**

```
You are a senior ML scientist specializing in tabular feature engineering and feature evaluation. Given dataset context and SHAP-based feature importances from a baseline model, your goal is to judge which of two candidate feature operations is more likely to improve the downstream metric when added to the current pipeline. Avoid label leakage; prefer complementary, non-redundant transformations to improve the model performance.
```

- **Instruction Prompt:**

```
Task: Choose the more promising feature operation between A and B

Dataset:
- Task type: [CLASSIFICATION_OR_REGRESSION]
- Metric: [ROC_AUC_OR_OTHER]
- Columns (name:type): [COLS_WITH_TYPES]
- Target: <TARGET_NAME>
- Notes (missingness, skew, constraints): <DATA_NOTES>

Baseline model + SHAP:
- Base model: <MODEL_NAME>
- Top SHAP features (name:score): <[(f1, s1), (f2, s2), ...]>

Recent performance feedback: [PERFORMANCE HISTORY]
Remaining iteration budget: [BUDGET]

Candidates:
A:
- name: <A_NAME>
- code: <A_CODE_SNIPPET_USING_df['...']>
- rationale: <WHY_THIS_MIGHT_HELP>

B:
- name: <B_NAME>
- code: <B_CODE_SNIPPET_USING_df['...']>
- rationale: <WHY_THIS_MIGHT_HELP>

Decision instructions:
- Prefer features that:
  1) Leverage high-SHAP columns sensibly (monotone transforms, interactions, ratios/differences, bins);
  2) Complement accepted features (diversity > redundancy);
  3) Are robust to outliers/missingness and unlikely to leak labels.
- Penalize features that:
  a) Duplicate existing ones; b) Are overly noisy/fragile;
Output format (JSON only):
{
  "choice": "A" | "B" ,
}
Return ONLY the JSON object.
```

E EXAMPLES OF LLM-PROPOSED FEATURE OPERATIONS

Below we provide several examples of LLM-proposed feature transformation operations selected by our algorithm. Each block shows the feature name together with its corresponding Python expression.

DAY_SINCE_FIRST_EVENT_WEIGHTED

```
feature = (0.5 * df['days_since_first_event_xxxxx_event_data']
           + 0.5 * df['days_since_first_event_yyyyy_event_data'])
```

WIFI_CLEANLINESS_BOOKING

```
feature = df['Inflight wifi service'] * df['Cleanliness'] * df['Ease of
Online booking']
```

DIGITAL_EXPERIENCE_TENSOR

```
gmean = (df['Inflight wifi service'] * df['Ease of Online booking']
          * df['Online boarding']) ** (1/3)
comfort = np.tanh((df['Seat comfort'] + df['Leg room service']) / 2.0)
feature = (gmean * (df['Cleanliness'] ** 0.5)) * comfort
```

BUSINESS_TRAVEL_CLEANLINESS_COMFORT

```
feature = (df['Type of Travel'] == 'Business travel') * \
           df[['Cleanliness', 'Seat comfort', 'Leg room service']].mean(
               axis=1)
```

AGE_WEIGHTED_HEALTH_INTERACTION

```
feature = (df['Age'] * (df['HighBP'] + df['HighChol'] + df['
HeartDiseaseorAttack'])) \
           / (1 + df['Smoker'] * df['BMI'])
```

LIFESTYLE_RISK_BALANCE_ENHANCED

```
feature = (df['Fruits'] + df['Veggies'] + df['PhysActivity']) / (
           df['Smoker'] + df['HvyAlcoholConsump'] + df['NoDocbcCost'] + 1
)
```

ACTIVITY_DIET_BALANCE

```
feature = (df['Fruits'] + df['Veggies'] + df['PhysActivity']) / (
           df['Smoker'] + df['HvyAlcoholConsump'] + 1
)
```

DIFF_WALK_HEALTH_INTERPLAY

```
feature = df['DiffWalk'] * df['BMI']
```

MULTI_AXIS_RISK_COMPOSITE

```
feature = (
    (df['Age'] * (df['HighBP'] + df['HighChol'] + df['
    HeartDiseaseorAttack']))
    / (1 + df['Smoker'] * (1 + df['BMI'])))
) * (
    (df['Fruits'] + df['Veggies'] + df['PhysActivity'] + 1)
    / (1 + df['HvyAlcoholConsump'] + df['NoDocbcCost'])
)
```